Structure Elucidation and Solution Conformation of the Glycopeptide Antibiotic Ramoplanose (UK-71,903): A Cyclic Depsipeptide Containing an Antiparallel β-Sheet and a β-Bulge†

Nicholas J. Skelton,‡ Margaret M. Harding,‡ Russell J. Mortishire-Smith,‡ Shirley K. Rahman,‡ Dudley H. Williams,*,‡ Michael J. Rance,§ and John C. Ruddock§

Contribution from the Cambridge Centre for Molecular Recognition, University Chemical Laboratory, Lensfield Road, Cambridge CB2 1EW, England, and Pfizer Central Research, Sandwich CT13 9NJ, England. *Received September 11, 1990*

Abstract: The primary structure of a new member of the group of antibiotics related to ramoplanin A2 (Ciabatti, R.; et al. *J. Antibiot.* **1989**, *42*, 254 and references therein) has been determined by a combination of chemical and spectroscopic methods. Ramoplanose (UK-71,903) differs from ramoplanin A2 in having a branched chain trisaccharide and a cis–trans N-terminal dienic fatty acid. The dominant solution conformation of the antibiotic aglycon was determined by using distance geometry and restrained molecular dynamics calculations. Input for these calculations was provided by 97 interresidue distance constraints obtained from nuclear Overhauser enhancement spectroscopy. Each of the resulting family of five structures contains two antiparallel β-strands connected by seven intramolecular hydrogen bonds and two reverse turns. One strand also incorporates a β-bulge. The stereochemistries of the amino acids along the peptide backbone induce curvature in the β-sheet, and a cleft is formed that may represent the active site.

Introduction

The determination of structure and conformation of an antibiotic is an important first step in addressing the problem of how its antimicrobial action is exerted. Armed with detailed information about the solution conformation of the antibiotic, hypotheses can be put forward concerning the means by which this interaction occurs.[1] In cases where the structures of the bacterial receptor and the antibiotic are known at a molecular level, it becomes possible to design rationally new analogues, in order to improve efficacy against bacteria without increasing harmful side effects.

This paper reports the elucidation of the primary structure and solution conformation of ramoplanose[2] (UK-71,903), a glycopeptide antibiotic that exhibits a high degree of activity against Gram-positive bacteria. The non-ribosomal origin of many peptide secondary metabolites often leads to the incorporation of nonstandard amino acids, blocked N-termini, and cyclic components.[3] Peptide antibiotics cyclized through lactone linkages with ring systems containing between 3 and 16 amino acids have been reported in the literature.[4] Within this range, examples containing smaller ring sizes are more numerous, and in almost all cases no details of conformation are reported. Ramoplanose has a molecular weight of 2713 Da,[5] and contains a macrocycle composed of 16 amino acids, of which 12 are nonstandard.

For our studies on ramoplanose, FAB-MS was used to determine the molecular weight of the antibiotic and to assess the outcome of microscale chemical derivatizations. Amino acid analysis was performed on hydrolysates of the antibiotic, and absolute stereochemistries of the α-amino acids were determined by chiral GC analysis.[6] NMR spectroscopy (DQF-COSY,[7] HOHAHA,[8] and NOESY[9]) was used to determine the primary sequence and to provide information about the solution conformation. The NMR-derived distance constraints were used in distance geometry[10] and restrained molecular dynamics calculations,[11] which allowed the solution conformation to be determined.

The antibiotic is found to be a cyclic depsipeptide of relatively high molecular weight (2713 Da with a molecular formula of $C_{125}H_{164}ClN_{21}O_{45}$). Three mannose units are attached to a 17-residue peptide core, while the N-terminus is blocked by a dienic fatty acid. Cyclization occurs from the C-terminal carboxyl group to the side chain hydroxyl group of the β-OH(Asn) at position 2 (Figure 1). The primary structure of the aglycon of ramoplanose closely resembles that of ramoplanin (A-16686).[12-14] While several different primary structures have been reported in this class, no solution conformation has been determined. Given the high degree of homology within this group of antibiotics, the solution conformation of ramoplanose described in this paper should provide structural information useful in the determination of the mode of action of all members of this class. Furthermore,

* To whom correspondence should be addressed.

† Abbreviations: FAB-MS, fast atom bombardment mass spectrometry; GC, gas chromatography; NMR, nuclear magnetic resonance; DQF-COSY double quantum filtered correlated spectroscopy; HOHAHA, homonuclear Hartman Hahn spectroscopy; NOESY, nuclear Overhauser enhanced spectroscopy; NOE, nuclear Overhauser enhancement; β-OH(Asn), β-hydroxyasparagine; HPLC, high-performance liquid chromatography; TFA, trifluoroacetic acid; 1(2)D, one (two) dimensional; FID, free induction decay; HPG, (hydroxyphenyl)glycine; CHP, (3-chloro-4-hydroxyphenyl)glycine; Orn, ornithine; Thr, *allo*-threonine; Ala, alanine; Asn, asparagine, Gly, glycine; Leu, leucine; Phe, phenylalanine; mu, mass units; MH^+, protonated molecular ion; DMSO, dimethyl sulfoxide; MAN, mannose.

‡ University of Cambridge.
§ Pfizer Central Research.

(1) For example, see: (a) Gale, E. F.; Cundliffe, E.; Waring, M. J.; Reynolds, P. E.; Richmond, M. H. *The Molecular Basis of Antibiotic Action*, 2nd ed.; John Wiley & Sons: New York, 1972. (b) Williams, D. H. *Acc. Chem. Res.* **1984**, *17*, 364.

(2) The name ramoplanose is derived from ramoplanin (see refs 12-14), which contains one fewer mannose unit.

(3) Kleinkauf, H.; von Döhren, H. *Annu. Rev. Biochem.* **1987**, *41*, 259.

(4) Kleinkauf, H.; von Döhren, H. *Curr. Top. Microbiol. Immunol.* **1987**, *91*, 129.

(5) Measured relative to $^{12}C = 12.000$. This is equivalent to a nominal mass of 2714 mu for the protonated species. All further masses of fragments and derivatives are given in nominal mass units (mu).

(6) Frank, H.; Nicholson, G. J.; Bayer, E. *J. Chromatogr. Sci.* **1977**, *15*, 174.

(7) Piantini, U.; Sørensen, O.; Ernst, R. R. *J. Am. Chem. Soc.* **1982**, *104*, 6800.

(8) (a) Braunschweiler, L.; Ernst, R. R. *J. Magn. Reson.* **1983**, *53*, 521. (b) Bax, A.; Davis, D. G. *J. Magn. Reson.* **1985**, *65*, 355. (c) Weber, P. L.; Sieker, L. C.; Samy, T. S. A.; Reid, B. R.; Drobny, G. P. *J. Am. Chem. Soc.* **1987**, *109*, 5842.

(9) (a) Jeener, J.; Meier, B. H.; Bachmann, P.; Ernst, R. R. *J. Chem. Phys.* **1979**, *71*, 4546. (b) Kumar, A.; Ernst, R. R.; Wüthrich, K. *Biochem. Biophys. Res. Commun.* **1980**, *95*, 1. (c) Macura, A.; Ernst, R. R. *Mol. Phys.* **1980**, *41*, 95.

(10) For a review, see: Kuntz, I. D.; Thomason, J. F.; Oshiro, C. M. *Methods Enzymol.* **1989**, *77*, 159.

(11) For a review, see: McCammon, J. A.; Harvey, S. C. *Dynamics of Proteins and Nucleic Acids*; Cambridge University Press: Cambridge, 1987.

(12) Cavalleri, B.; Pagani, H.; Volpe, G.; Selva, E.; Parenti, F. *J. Antibiot.* **1984**, *37*, 309.

(13) Kettenring, J. K.; Ciabatti, R.; Winters, G.; Tamborini, G.; Cavalleri, B. *J. Antibiot.* **1989**, *42*, 268.

(14) Ciabatti, R.; Kettenring, J. K.; Winters, G.; Tuan, G.; Zerilli, L.; Cavalleri, B. *J. Antibiot.* **1989**, *42*, 254.

0002-7863/91/1513-7522$02.50/0

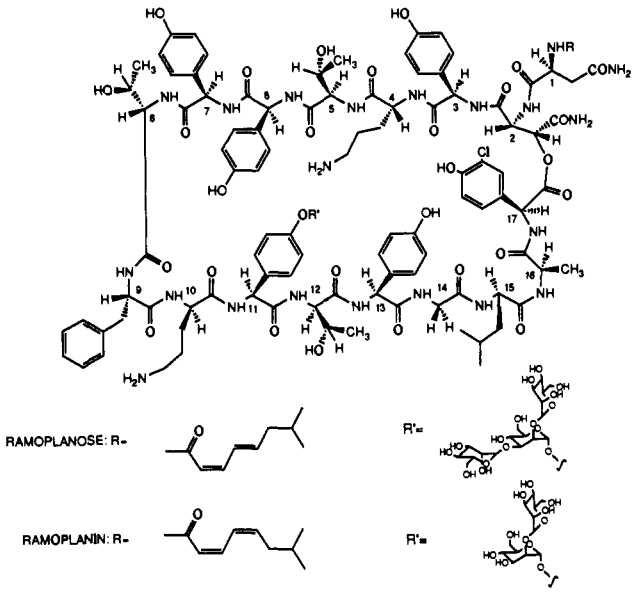

Figure 1. Structures of ramoplanin (A-16686 factor A2) and ramoplanose (UK-71,903).

ramoplanose appears to represent the first example of stable extended β-sheet structure in a large cyclic peptide.

Experimental Section

Isolation. Ramoplanose was produced by fermentation by a new Actinoplanes species. After the mycelial cake was washed with acetone, the crude product was extracted from the cake by washing with methanol/hydrochloric acid (1:4, pH 2.5). The antibiotic was subjected to preparative HPLC (Waters Prep-500 system, acetonitrile/potassium dihydrogen phosphate (0.1 M), 200 mL/min). Combined fractions were desalted by adsorption onto XAD2 resin and elution with 50% aqueous acetone. Final purification was effected by HPLC (Waters μ-Bondapak 10 × 300 mm ODS-2, acetonitrile/25 mM ammonium acetate (28:72)). Inorganic salts were removed by further elution with acetonitrile/water (1:1) (0.1% TFA).

Carbohydrate Analysis. Carbohydrate analysis was performed by using the methods described by McGahren et al.[15] Mannose was determined to be the only sugar present in the antibiotic.

FAB Mass Spectrometry. FAB-MS[16] of ramoplanose in *m*-nitrobenzyl alcohol was acquired on a VG 70 SE mass spectrometer (VG 11-250 data system) equipped with a cesium gun and calibrated with CsRbI. Spectra were recorded at resolution 3000 for the protonated molecular ion and resolution 5000 for the accurate mass. Analysis of pulse hydrolysis and derivatization experiments was carried out on a Kratos MS-50-TC spectrometer equipped with an Ion Tech gun accelerating xenon atoms to 6-9 keV for sample bombardment. Spectra were recorded in positive ion mode using 10–20 nmol of compound dissolved in 2–3 μL of glycerol with 5% v/v 15-c-5 crown ether and were calibrated with characteristic matrix cluster ions.

Hydrolysis and Derivatization Studies. Hydrolyses and derivatization reactions were performed under nitrogen on 0.5–1-mg antibiotic samples. For pulse acid hydrolysis, sequanal-grade HCl (6 N, 100 μL) was added and the sample heated at 100 °C for 5–30 min and then cooled and lyophilized. Base hydrolyses were performed at room temperature in NaOH (1 N, 100 μL) for 20 min and then quenched with HCl (2 N), buffered with ammonium acetate (1 N, 20 μL), desalted by elution through a Sep-Pak cartridge with acetonitrile/water mixtures containing 0.1% TFA, and lyophilized. Samples dissolved in methanol (200 μL) and acetic acid (20 μL) were hydrogenated over palladium on charcoal catalyst (5%, 1 mg) under hydrogen for 6 h.

Amino Acid Analysis. Peptide samples were hydrolyzed at 110 °C by the vapor of 6 M HCl containing 0.1% 2-mercaptoethanol and 1 mM phenol under argon for 24–96 h. Amino acid composition was determined on an LKB 4400 amino acid analyzer using ninhydrin detection.

Chiral GC Analysis of Amino Acids. GC was carried out according to the protocol described by Nutkins et al.[17] on samples of antibiotic (2 mg) hydrolyzed in HCl (2 N, 200 μL) under nitrogen at 100 °C for 24 h. Standard amino acid samples were coinjected to verify identification. The optical isomers of alanine, threonine, leucine, phenylalanine, and aspartic acid were analyzed as their *N,O*-trifluoroacetyl isopropyl esters and β-hydroxyaspartic acid as its *N*-trifluoroacetyl propyl ester. The optical isomers of (*p*-hydroxyphenyl)glycine, (3-chloro-4-hydroxyphenyl)glycine, and ornithine were analyzed as their *N,O*-pentafluoropropionyl propyl esters.

NMR Spectroscopy. Proton NMR spectra were recorded with Bruker AM-400 and AM-500 spectrometers equipped with Aspect 2000 computers. Samples (5–10 mg) were dissolved in D_2O (500 μL; Aldrich; 99.95 atom %) and DCl (20%, 10 μL; Aldrich) and immediately frozen and lyophilized. These samples were dried in vacuo over phosphorus pentoxide before the antibiotic was dissolved in D_2O (500 μL). Spectra were recorded over spectral widths of 4000 or 5000 Hz (at 400 and 500 MHz, respectively) with quadrature detection. Chemical shifts were measured relative to internal (3-trimethylsilyl)-1-propanesulfonate at 0.0 ppm. 2D proton NMR spectra were acquired in the phase-sensitive mode using quadrature detection in f_2, and with the time proportional phase incrementation method of Marion and Wüthrich in f_1.[18] Data sets resulting from 400–512 increments of t_1 were acquired (and zero filled to 1024 points), with each FID composed of 2048 data points. The sum of acquisition time and recycle delay between transients was typically 1.5–2.0 s, and 64 or 96 transients were recorded for each increment of t_1. NOESY spectra were recorded with mixing times of 200–400 ms, varied by 20–30 ms between t_1 values to minimize zero quantum artifacts.[19] HOHAHA spectra were recorded by using a 5-kHz spin locking field; an MLEV-17 sequence was used to provide the isotropic mixing, and the spin locking field was applied for 50 or 100 ms.[8] The final data sets were multiplied by Lorentzian–Gaussian functions before Fourier transformation. Phase-coherent solvent suppression was achieved in H_2O solution by a DANTE[20,21] sequence (pulse width 0.8–1.0 μs and interpulse delay 180–200 μs) applied for 1.0 s before the start of each transient, and during the mixing time in the NOESY experiments. Solvent suppression was not applied during the isotropic mixing period of the HOHAHA spectra in water. 2D spectra in water were usually acquired with 256 increments in t_1 (zero filled to 1024 data points) with 96 or 128 transients for each increment.

$^3J_{NH\text{-}C\alpha H}$ coupling constants were extracted from resolution-enhanced 1D spectra acquired from H_2O solution. Spectra were zero-filled to achieve a digital resolution of 0.4 Hz/point. Analysis of the fatty acid DQF-COSY cross-peak fine structure was performed on a spectrum zero filled to 0.8 Hz/point in f_2, and 1.1 Hz/point in f_1. These cross-peaks were simulated by using the program SPINNER (Mark Rance, unpublished work). Spectral widths and digital resolutions within the simulations were chosen to match the data as closely as possible.

Computational Molecular Modeling. DG and rMD calculations were performed on a Microvax 3600 computer. Routinely, a DG calculation required 1.5 h of cpu time per structure, while a rMD calculation could be completed in 6 h of cpu time. Distance geometry calculations were performed with the DGEOM package of Blaney.[22] Input constraints consisted of those interatomic distances fixed by the covalent geometry of the peptide aglycon, combined with experimental constraints generated by NOE analysis. NOEs were quantified into three regimes[23] by inspection of NOESY spectra run at varying mixing times; strong (1.8–2.7 Å), medium (1.8–3.5 Å), and weak (1.8–5.0 Å). Reference for this quantitation was provided by NOEs observed between the 2,6- and 3,5-protons of aromatic amino acids, whose separation is fixed at 2.51 Å. A total of 97 interresidue NOEs were identified and used as distance constraints. Input coordinates were taken from the peptide in a linear β-strand conformation. Minimum approach distances between atoms were set to the sum of van der Waal's radii. Improper constraints were imposed to maintain chirality and hold aromatic rings planar, and charges were not included on the Orn side chains. Structures generated by this method were subjected to 500 iterations of restrained minimization in the AMBER force field,[24] where harmonic restraints were imposed

(15) McGahren, W. J.; Leese, R. A.; Barbatsci, F.; Morton, G. O.; Kuck, N. A.; Ellestad, G. A. *J. Antibiot.* **1983**, *36*, 12.
(16) Barber, M.; Bordoli, R. S.; Sedgwick, R. D.; Tyler, A. N. *Nature* **1981**, *293*, 270.
(17) Nutkins, J. C.; Mortishire-Smith, R. J.; Packman, L. C.; Brodey, C. L.; Rainey, P. B.; Johnstone, K.; Williams, D. H. *J. Am. Chem. Soc.* **1991**, *113*, 2621.
(18) Marion, D.; Wüthrich, K. *Biochem. Biophys. Res. Commun.* **1983**, *113*, 967.
(19) Rance, M.; Bodenhausen, G.; Wagner, G.; Wüthrich, K.; Ernst, R. R. *J. Magn. Reson.* **1985**, *62*, 497.
(20) Zuiderweg, E. R. P.; Hallenga, K.; Olejniczak, E. T. *J. Magn. Reson.* **1986**, *70*, 336.
(21) Morris, G. A.; Freeman, R. *J. Magn. Reson.* **1978**, *29*, 433.
(22) Written by J. M. Blaney and G. M. Crippen, University of Michigan, 1986.
(23) Braun, W.; Bösch, C.; Brown, L. R.; Gō, N.; Wüthrich, K. *Biochem. Biophys. Acta* **1981**, *667*, 377.

Table 1. Amino Acid Content of Ramoplanose

amino acid	amino acid analysis[a]	NMR quantitation[b]	stereochemistry[c]
alanine	1.01	1	D
aspartic acid	1.00	1	L
β-hydroxyaspartic acid	0.44	1	L
glycine	1.02	1	
leucine	0.96	1	L
ornithine	1.95	2	D
phenylalanine	1.12	1	L
(*m*-chloro-*p*-hydroxyphenyl)glycine	0.87	1	L
(*p*-hydroxyphenyl)glycine	4.00	5	2D + 3L
allo-threonine	2.01	3	2D + 1L

[a] Quantitation relative to one aspartic acid residue. [b] NMR quantitation derived from the number of appropriate spin systems observed in DQF-COSY spectra. [c] Absolute stereochemistries as determined by chiral GC.

between protons for which NOE constraints existed. Pseudoatom constraints were used for nonstereospecifically assigned protons. All interproton contacts expected to result in an NOE were calculated, and those structures which best satisfied the NOE data were subjected to restrained molecular dynamics using the XPLOR package of Brünger et al.[25] Force field parameters for HPG, CHP, and Orn residues were generated by modifying those for tyrosine and lysine in the standard XPLOR residue library. Force constants for stretching and bending and torsional terms not included in the XPLOR parameter set were modified from the MM2 force field,[26] scaled to be consistent with XPLOR parameters. Improper constraints were applied to asymmetric carbon atoms to maintain chirality and to hold the fixed stereochemistry of the N-terminal fatty acid. Structures were heated to 900 K during 2 ps by the temperature-regulated MD algorithm of Berendsen[27] with the default friction coefficient of 100 ps^{-1}. Initial velocities were generated from a Maxwell distribution at 20 K. Equilibration at 900 K for 2 ps was followed by a 4-ps cooling period to 0 K. Hydrogen-bonding constraints were then included on the basis of the apparent fold of the peptide in the generated structures, combined with data on slowly exchanging amide protons, and the structures put through a further restrained dynamics run using the protocol given above. Finally, structures were minimized without restraint for 500 iterations in the AMBER force field.

Results

Amino Acid Analysis. The results of quantitative amino acid analysis conducted on acid hydrolysates of ramoplanose are summarized in Table I. The choice of unusual amino acid standards (Orn, Thr, HPG, and CHP) was guided by the initial NMR studies in D_2O, which identified spin systems compatible with these residues. Comparison of the retention times of amino acid standards identified all residues listed in Table I except β-OH(Asp), which was identified by GC analysis of the *N,O*-trifluoroacetyl propyl esters of the ramoplanose hydrolysate. Better quantitation of the number of each residue present was provided by NMR; discrete spin systems from five HPG, three Thr, and two Orn residues were identified, bringing the total number of residues to seventeen.

Amino Acid Stereochemistry. GC analysis of the derivatized hydrolysate of ramoplanose using a chiral stationary phase permitted the resolution and identification of the L isomers of Leu, Asp, β-OH(Asp), Phe, and *allo*-Thr, and the D isomers of Ala and *allo*-Thr (Table I). The chiralities of Orn (2 × D), CHP (L), and HPG residues (2 × D and 3 × L) were established by analysis of the more volatile *N,O*-pentafluoropropionyl isopropyl esters of the ramoplanose hydrolysate (Table I).

FAB Mass Spectrometry of Derivatives of Ramoplanose. The positive ion spectra of ramoplanose exhibited a MH^+ with an accurate mass determined to be 2715.349 at high resolution (corresponding to a nominal integral mass of 2714 mu for the protonated ion). Less abundant fragment ions were observed at

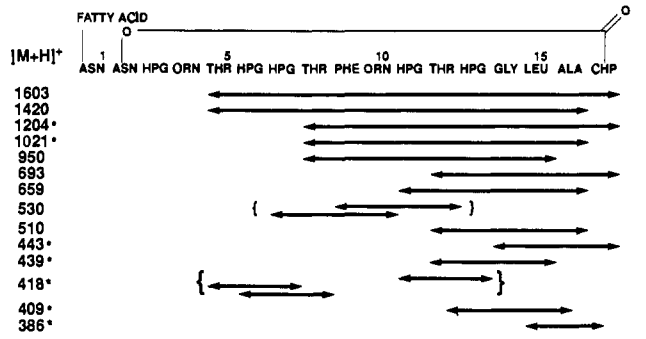

Figure 2. FAB-MS fragments observed after pulse hydrolysis of ramoplanose (6 N HCl, 15–30 min, 100 °C). Asterisks indicate ions that are also observed after pulse acid hydrolysis of the lactone opened antibiotic.

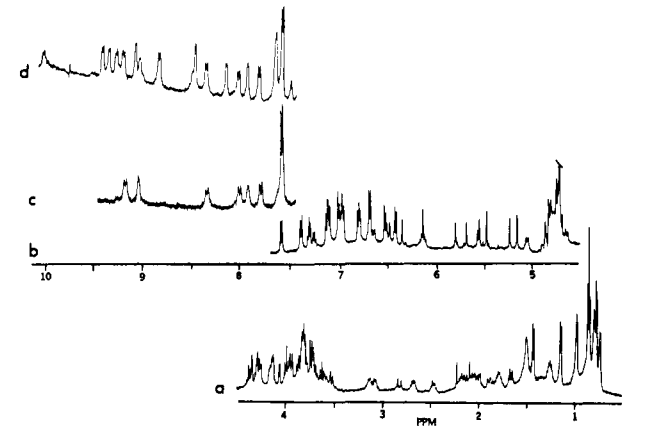

Figure 3. 500-MHz proton NMR spectrum of ramoplanose in aqueous solution, 295 K: (a) high-field region in D_2O, (b) low-field region in D_2O, (c) low-field region in D_2O before complete exchange of amide protons, (d) low-field region in 90% H_2O/10% D_2O.

162, 324, and 486 mu below the molecular ion, suggesting the presence of three hexoses. This was confirmed by neutral sugar analysis where only D-mannose was observed.

Mild acid hydrolysis conditions (1 N HCl, 100 °C, 5–30 min) produced an abundant MH^+ at 2228 mu, consistent with removal of three sugar units. Harsher conditions (6 N HCl, 105 °C, 10 min) resulted in MH^+ at 2228, 2094, and 1979 mu. The loss of 134 mu to give rise to an ion at 2094 mu is consistent with the loss of a C_9 dienic fatty acid (−136 mu—see below) and the hydrolysis of two amides to the corresponding acid functionalities (+2 mu), while the further loss of 115 mu is attributable to removal of aspartic acid (asparagine prior to hydrolysis) from the N-terminus to produce an ion at 1979 mu. Catalytic hydrogenation of the antibiotic resulted in a signal at 2718 mu, which is indicative of the reduction of two double bonds, a result consistent with the conjugated diene assigned in the NMR spectrum (see below).

Hydrolysis of ramoplanose under basic conditions (1 N NaOH, 25 °C, 20 min) afforded a product with an abundant MH^+ at 2732 mu, which was rationalized in terms of breaking a lactone linkage, providing evidence for a cyclic depsipeptide. Intact ramoplanose was reduced with $LiBH_4$ and the hydrolysis product derivatized with trifluoroacetic anhydride and HCl/propanol. GC analysis revealed an absence of CHP, and the appearance of a new compound that was identified as 2-amino-2-(3-chloro-4-hydroxyphenyl)ethanol by coinjection with an authentic sample. Hence, the carboxyl group of the lactone linkage is provided by the CHP residue.

With the benefit of additional sequence information obtained from the NMR spectra (see below), it is possible to assign the ions observed in the FAB-MS spectra of the hydrolysis products (Figure 2) to particular peptides. The majority of the ions present above *m/z* 350 could be assigned to specific sequences containing from three to twelve residues. While this is not conclusive proof

(24) Weiner, S. J.; Kollman, P. A.; Nguyen, D. T.; Case, D. A. *J. Comput. Chem.* **1986**, *7*, 230.
(25) Brunger, A. T.; Clore, G. M.; Gronenborn, A. M.; Karplus, M. *Proc. Natl. Acad. Sci. U.S.A.* **1986**, *83*, 3801.
(26) Burkert, U.; Allinger, N. L. *Molecular Mechanics*; American Chemical Society: Washington, DC, 1982.
(27) Berendsen, H. J. C.; Postma, J. P. M.; van Gunsteren, W. F.; DiNola, A.; Haak, J. R. *J. Chem. Phys.* **1984**, *81*, 3684.

Table II. Chemical Shift (ppm), Amide Proton Temperature Dependence and Amide Proton Exchange Data for Ramoplanose in Aqueous Solution at 295 K

fatty acid	2 = 5.5	3 = 6.50	4 = 6.96	5 = 6.13	6/6′ = 2.00	7 = 1.65	8 = 0.86 8′ = 0.88
				ring position			
		1	2	3	4	5	6
mannose 1		5.62	4.28	4.27	3.96	3.54	3.50 3.77
mannose 2		5.23	4.14	3.79	3.69[a]	3.92[a]	
mannose 3		5.16	4.05	3.84	3.78[a]	3.68[a]	3.60[a] 3.74[a]

residue	NH[b]	αCH	βCH	γCH	δCH	$J_{\alpha CH-NH}$ (Hz)	$\Delta\delta/T$[e] (ppb K^{-1})
Asn1 (L)	8.13	4.60	1.62 2.09		6.19[c] 6.49[c]		7.3
β-OH(Asn2) (L)	8.37	5.55	5.80		7.43[c] 6.94[c]	9.5	2.6
HPG3 (D)	10.03	6.36		7.59	7.10	8.7	7.3
Orn4 (D)	9.30	4.30	1.35 1.46	1.24	2.47 2.67	9.1	3.1
Thr5 (Da)	7.64	4.35	4.15	1.16		*d*	*d*
HPG6 (L)	8.83	6.79		6.67	6.43	9.6	5.6
HPG7 (D)	9.08	5.49		6.67	6.51	3.1	5.6
Thr8 (La)	8.45	3.84	3.95	0.79		*d*	*d*
Phe9 (L)	7.64	4.16	1.88 1.97		2/6 = 7.01 3/5 = 7.30 4 = 7.25	*d*	*d*
Orn10 (D)	7.81	5.05	2.07 2.19	1.76 1.76	3.08 3.14	9.2	2.8
HPG11 (L)	9.42	6.99		7.38	6.95	8.3	6.9
Thr12 (Da)	9.21	4.77	4.00	0.99		9.5	4.3
HPG13 (L)	9.04	6.15		7.12	6.79		5.6
Gly14	7.94	2.82 3.91					2.0
Leu15 (L)	8.45	4.25	1.49	1.49	0.76 0.81	*d*	*d*
Ala16 (D)	9.34	4.37	1.44			6.1	2.3
CHP17 (L)	8.02	4.74			2 = 6.46 5 = 7.00 6 = 6.72	10.1	2.5

[a] Tentative assignment (see text). [b] Underlined amide resonances undergo slow exchange with solvent. [c] Arbitrary assignment as no intraresidue NOEs were observed to allow an unambiguous sequence-specific assignment of the two side chain $N^{\delta}H_2$ groups. [d] Amide resonance overlap of Thr5 with Phe9 and Thr8 with Leu15 precludes the measurement of $^3J_{\alpha NH}$ and temperature coefficients. [e] Measured over the range 275–310 K.

that the sequence is correct, it does provide very strong supporting evidence. In this capacity, FAB-MS is playing a role similar to its use in "FAB mapping" of protein digests.[28]

NMR Spectroscopy. In DMSO and DMSO/TFA solution, the ^1H NMR spectra of ramoplanose exhibit poor spectral resolution and broad line width over the temperature range 298–350 K. However, in aqueous solution, well-resolved resonances of low line width were obtained. The NMR spectrum obtained in aqueous solution is presented in Figure 3. Of particular interest are the seven amide resonances observed in D_2O solution (Figure 3c), which are observable for a period of 7–10 days after initial dissolution of the sample. The temperature dependence of amide proton chemical shifts was determined from spectra recorded in H_2O solution over the temperature range 275–310 K by using a modified Hore 1-3-3-1 selective excitation sequence (Table II).[29] Solvent suppression by this method confirmed that presaturation was not attenuating any amide resonances by fast exchange with the solvent. All of the amide protons that underwent slow chemical exchange with D_2O (Figure 3c) had lower temperature coefficients than the amide protons that exchanged rapidly with D_2O (2–6 ppb K^{-1} and >7 ppb K^{-1}, respectively).

Identification of Amino Acid Spin Systems. In general, the majority of resonances in the peptide backbone and aliphatic side chains could be identified by the scalar coupling networks observed in the DQF-COSY spectrum acquired in D_2O solution.[30] In several cases, severe overlap problems were resolved by using the relayed connectivities observed in the HOHAHA spectrum. Similarly, the amide proton resonances were assigned in spectra acquired from H_2O solution either by direct connectivity to $C^{\alpha}H$ in the DQF-COSY or by HOHAHA relay to resonances further along the side chain. In particular, the $C^{\alpha}H$ protons of Ala16, Leu15, Orn4, and Thr5 are all close in chemical shift, and those of Orn10 and Thr12 are sufficiently close to the water resonance that direct NH–$C^{\alpha}H$ correlations are obscured by imperfect solvent suppression. The $C^{\alpha}H$ of CHP17 also lies directly under the water resonance, but NH–$C^{\alpha}H$ correlations could be observed in D_2O experiments owing to the slow rate of exchange of this amide proton with solvent. Inspection of the NOESY acquired from H_2O solution also revealed two intense cross-peaks not present in the D_2O data (6.19–6.49 ppm, and 6.94–7.43 ppm). These resonances were assigned to the side chain NH_2 groups of Asn and β-OH(Asn). No further NOEs were observed to these resonances; hence, they could not be assigned in a sequence-specific manner.

The seven aromatic ring systems were assigned by examination of the aromatic region of the DQF-COSY spectrum. Five pairs of doublets, corresponding to 1,4-disubstituted rings of the HPG residues, were observed. All of these rings are able to undergo relatively rapid 180° ring flips about their C^{α}–C^{β} bond as evi-

(28) (a) Gibson, B.; Biemann, K. *Proc. Natl. Acad. Sci. U.S.A.* **1984**, *49*, 26. (b) Naylor, S.; Findeis, A. F.; Gibson, B. W.; Williams, D. H. *J. Am. Chem. Soc.* **1986**, *108*, 6359.

(29) (a) Hore, P. J. *J. Magn. Reson.* **1985**, *54*, 146. (b) Galloway, G. J.; Haseller, L. J.; Marshman, M. F.; Williams, D. H.; Doddrell, D. M. *J. Magn. Reson.* **1987**, *74*, 184.

(30) Wüthrich, K. *NMR of Proteins and Nucleic Acids*; John Wiley & Sons: New York, 1986; pp 117–129, 162–199.

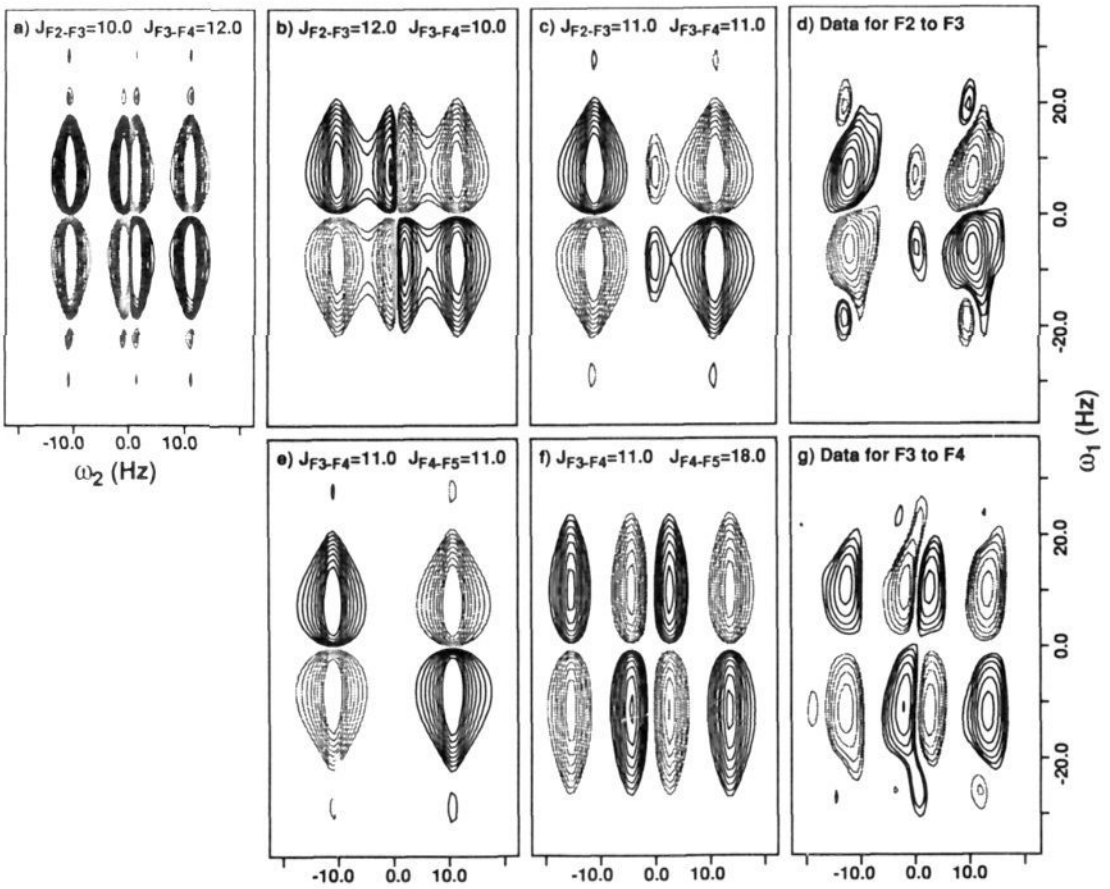

Figure 4. Real and simulated DQF-COSY cross-peaks for the dienic fatty acid group of ramoplanose. The information in the top row pertains to $^3J_{F3-F4}$, and the lower to $^3J_{F4-F5}$. Negative contours are denoted by shaded lines. The cross-peaks F2 to F3 (a–d, F2 in the f_1 dimension) and F3 to F4 (e–g, F3 in the f_1 dimension) are depicted. The values of $^3J_{F2-F3}$, $^3J_{F3-F4}$, and $^3J_{F4-F5}$ used in the simulations are given in each box. The best simulation is presented immediately to the left of the real data. The real data (d and g) were collected at 500 MHz with an acquisition time of 330 ms and a t_{1max} of 65 ms. Data were processed with sine-bell apodization (shifted 60° in f_2 and 75° in f_1) prior to Fourier transformation and zero-filled to give a final digital resolution of 0.79 Hz/point in f_2 and .12 Hz/point in f_1. The simulated spectra have a digital resolution of 0.83 Hz/pt in both dimensions, and were produced with an acquisition time of 300 ms and a t_{1max} of 61 ms. Truncation was curtailed by multiplication with sine-bells (shifted 60° in f_2 and 75° in f_1). Exponential line broadening of 3 Hz in f_2 and 4 Hz in f_1 was also applied to reproduce the experimental line widths.

denced by only two magnetically distinct proton resonances present in each ring (A_2X_2 spin systems). Spin systems corresponding to the ring system of phenylalanine, and a 1,3,4-trisubstituted ring (CHP), were also identifiable. Connectivities were established between the aromatic ring protons and their backbone protons by NOESY experiments acquired in D_2O solution. The chemical shifts of all resonances are listed in Table II, together with their NH–C$^\alpha$H coupling constants and amide proton temperature coefficients where available.

Groups Attached to the Peptide Core. The COSY spectrum in D_2O showed a linear system of four coupled spins (F2, F3, F4, and F5) in the downfield region of the spectrum, with further correlations observed in the HOHAHA spectrum from F5 to several upfield protons (a methylene, F6/6′; a methine, F7; and a geminal dimethyl group, F8 and F8′). The chemical shifts and splitting patterns of these resonances are indicative of a conjugated diene that is part of an extended hydrocarbon chain, i.e., part of a dienic fatty acid. This assignment is consistent with the results of hydrogenation experiments (see above). $^3J_{F2-F3}$ was measured directly from the 1D spectrum as 11.2 Hz. Due to partial coincidence with other resonances, $^3J_{F3-F4}$ and $^3J_{F4-F5}$ cannot be measured directly from the 1D spectrum. However, it is possible to estimate their size from the fine structure of cross-peaks in a DQF-COSY spectrum. Although the extraction of coupling constants from COSY cross-peaks is prone to systematic error,[31] the cross-peak simulations shown in Figure 4 clearly indicate that

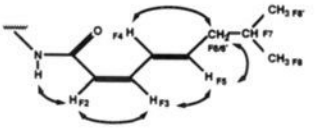

Figure 5. Structure of the fatty acid blocking the N-terminus of ramoplanose. Arrows denote NOEs observed within the fatty acid moiety.

the observed fine structure can only occur if $^3J_{F2-F3} \approx {}^3J_{F3-F4} < {}^3J_{F4-F5}$. Coupling constants of 11, 11, and 18 Hz for $^3J_{F2-F3}$, $^3J_{F3-F4}$, and $^3J_{F4-F5}$, respectively, indicate a cis stereochemistry for the F2–F3 bond and a trans geometry about the F4–F5 bond.[32] The NOEs observed between these protons (Figure 5) confirm the cis/trans stereochemistries, and also indicate that the F3–F4 bond is predominantly in a *transoid* conformation. An NOE from F2 to the amide proton of Asn1 indicates that the fatty acid blocks the N-terminus of this residue.

Three doublets ($J < 2$ Hz) close to 5.5 ppm and coupled to peaks further upfield were assigned to the anomeric protons of the three mannose units expected from FAB-MS fragments and carbohydrate analysis. Starting from the anomeric resonances, coupling pathways were followed in the DQF-COSY, with relayed connectivities present in the HOHAHA spectrum helping to circumvent some of the severe overlap problems among the sugar protons. All resonances of MAN1 were firmly assigned, while

(31) Neuhaus, D.; Wagner, G.; Vasák, M.; Kägi, J. H. R.; Wüthrich, E. *Eur. J. Biochem.* **1985**, *151*, 257.

(32) Silverstein, R. M.; Bassler, G. C.; Morrill, T. C. *Spectroscopic Identification of Organic Compounds*; John Wiley & Sons: New York, 1981; pp 205–206.

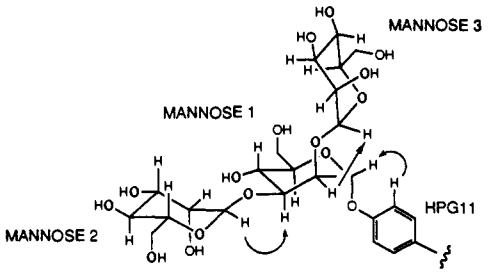

Figure 6. Structure of the trisaccharide found in ramoplanose. Arrows denote observed NOEs that were used to determine the carbohydrate structure.

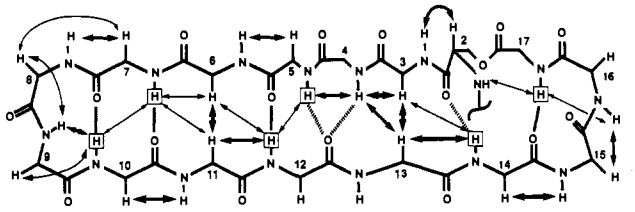

Figure 7. Hydrogen-bonding network suggested by distance geometry and dynamics calculations. Side chains are omitted for clarity. The hatched lines indicate the proposed hydrogen bonds, while the arrows indicate the observed NOEs (the relative intensity of the NOE is indicated by the thickness of the arrow). Amide protons surrounded by boxes exchange slowly with solvent. These hydrogen bond contraints were imposed in the final dynamics simulations.

the resonance positions of protons in the 4, 5, 6, and 6′ positions of MAN2 and MAN3 are less certain. The chemical shift assignments are listed in Table II. No intraresidue H_1 to H_3 NOEs (or H_1 to H_5 of the fully assigned MAN1) were observed, indicating that all three sugars are present as their α-anomers. The positions of the sugars within the antibiotic were determined by examination of NOEs to anomeric protons, viz., $MAN1_{H1}$ to $HPG11_{3,5}$, $MAN2_{H1}$ to $MAN1_{H3}$, and $MAN3_{H1}$ to $MAN1_{H2}$. Thus, the sugars are attached as a branched trisaccharide to HPG11 (Figure 6).

Primary Structure. In the absence of unambiguous primary sequence information from the FAB-MS studies, NOE data were used both to determine the primary sequence of the aglycon and to make the sequential resonance assignments. This process relies on the observation of NOEs from the amide proton of one residue to the amide C^{α} and C^{β} protons of the preceding residue in the peptide chain. Studies of protein structure have shown that the majority of amide–amide, amide–$C^{\alpha}H$ and amide–$C^{\beta}H$ NOEs occur between adjacent residues.[33] In ramoplanose, a sequence of such NOEs can be traced from residue 1 to residue 17 (Table IV). Further, a d_{NN} NOE is also observed from β-OH(Asn) to CHP17. This NOE, combined with the knowledge that CHP17 is involved in a lactone linkage (see above), indicates that cyclization occurs from O^{β} of residue 2 to the carboxyl group of CHP17. As described above, the covalent structure determined from this analysis is in complete agreement with all fragmentation and pulse hydrolysis data obtained by FAB-MS (Figure 2).

The large number of intense $d_{\alpha N}(i,i+1)$ NOEs and scarcity of $d_{NN}(i,i+1)$ NOEs suggest that the backbone of the antibiotic is largely in an extended structure. Additional evidence for this is provided by the intense $d_{\alpha\alpha}(i,j)$ NOEs from residue 3 to 13, and from 6 to 11, which indicate the presence of an antiparallel β-sheet motif (Figure 7). The constrained nature of the backbone within this β-sheet make it possible to resolve the ambiguities in the absolute stereochemistry of the Thr and HPG residues by considering side chain–side chain NOEs. Given the absolute stereochemistries of β-OH(Asn2), Orn4, Phe9, Orn10, Leu15, Ala16, and CHP17, the observed side chain–side chain NOEs (Table III and Figure 8) are only compatible with one set of absolute stereochemistries. The complete covalent structure of ramoplanose is summarized in Figure 1, while the absolute stereochemistries are listed in Table II.

Table III. Interresidue NOEs for Ramoplanose in Aqueous Solution

proton		NOEs observed[a]
Asn1	NH	F2 (m)
	α	β-OH (Asn2) NH (s), Leu15α (m), Leu15β (s)
	β	Gly14 NH (s), β-OH(Asn2) NH (s)
β-OH(Asn2)	NH	CHP17 NH (s), Gly14 NH (s)
	α	HPG3 NH (m), $HPG3_{2,6}$ (m)
	β	HPG3 NH (m), $HPG3_{2,6}$ (m), $HPG3_{3,5}$ (s)
HPG3	α	Orn4 NH (l), HPG13α (l), $HPG13_{2,6}$ (l), $CHP17_2$ (s),
	2,6	Orn4 NH (s), HPG13α (m), $CHP17_2$ (s), HPG7 NH (s)
	3,5	HPG7 NH (s), $CHP17_2$ (s)
Orn4	NH	Thr5 NH (m), HPG13α (m), $HPG13_{3,5}$ (s)
	γ	Thr5 NH (m), Thr5α (s), Thr5γ (s), Thr12γ (s), $HPG13_{2,6}$ (s), $HPG13_{3,5}$ (s)
	δ	$HPG13_{2,6}$ (s), $HPG13_{3,5}$ (s)
Thr5	NH	Thr12γ (s), Thr12 NH (s)
	α	HPG6 NH (m)
	γ	HPG6 NH (m), HPG6α (s), $HPG6_{2,6}$ (m), $HPG6_{3,5}$ (s), $HPG11_{2,6}$ (m), $HPG11_{3,5}$ (m), Thr12γ (s)
HPG6	NH	$HPG7_{2,6}$ (s)
	α	Thr5γ (s), HPG7 NH (m), HPG11a (l), $HPG11_{2,6}$ (s)
	2,6	Thr5γ (m), HPG11α (m), $HPG11_{2,6}$ (s), Thr12 NH (m)
	3,5	Thr5γ (s)
HPG7	NH	Orn10 NH (s), HPG11α (s)
	α	Thr8 NH (m), Thr8α (s)
	2,6	Thr8 NH (m), Orn10β (s), HPG11α (m)
	3,5	HPG11α (l)
Thr8	α	Phe9 NH (s)
	β	Phe9 NH (s)
	γ	Phe9 NH (s), Phe9β (s), $Phe9_{2,6}$ (s), $Phe9_{3,5}$ (s), Orn10γ (s)
Phe9	NH	Orn10 NH (m)
	α	Orn10 NH (s)
Orn10	α	HPG11 HN (m), $HPG11_{2,6}$ (s), $HPG11_{3,5}$ (s)
	β	HPG11 NH (s), $HPG11_{2,6}$ (s)
HPG11	α	Thr12 NH (m)
	2,6	Thr12 NH (m), Thr12β (m), Thr12γ (m)
	3,5	Thr12β (s), Thr12γ (s), mannose 11 (l)
Thr12	γ	HPG13 NH (m), $HPG13_{2,6}$ (s), $HPG13_{3,5}$ (s)
HPG13	α	Gly14 NH (l)
	2,6	Gly14 NH (m)
Gly14	α	Leu15 NH (l)
Leu15	NH	Ala16β (s)
	α	Ala16 NH (m), CHP17 NH (s)
	δ	Ala16 NH (s), Ala16β (m), F8/8′ (s)
Ala16	NH	CHP17 NH (s)
	β	CHP17 NH (s), F8/8′ (m)

[a] Data obtained at 500 MHz in D_2O at 295 K with a mixing time of 250 ms, except for NOEs to NH protons, which were observed in 90% H_2O/D_2O solution at 295 K with a 400-ms mixing time. Size of cross-peaks quantitated by relative intensities: s = small, m = medium, l = large. NOEs are tabulated in one direction only.

Solution Conformation. The solution conformation of ramoplanose was determined by a combination of distance geometry and molecular dynamics calculations using the complete set of NOE data listed in Table III. The absence of $d_{NN}(i,i+1)$ connectivities was taken as strong evidence against sections of the α-helix in the secondary structure. Given the mixed stereochemistry of ramoplanose, this is hardly surprising; steric interactions between the side chains of L and D residues at i and $i+3$ positions disfavor α-helix formation. A further indication of the type of secondary structure present in the antibiotic is provided by the vicinal coupling constants $^3J_{\alpha NH}$ (Table II). Values of $^3J_{\alpha NH} < 6.0$ Hz for helical residues and $^3J_{\alpha NH} > 8.0$ Hz for residues in the β-structure are typically observed.[30] Thus, the eight observed values of $^3J_{\alpha NH}$ greater than 8.0 Hz are consistent with the β-structure in ramoplanose. The overall fold of the peptide is apparent from inspection of interresidue NOE connectivities

(33) Billeter, M.; Braun, W.; Wüthrich, K. *J. Mol. Biol.* **1982**, *174*, 321–346.

Table IV. Sequential NOEs Used To Make Sequence-Specific Assignments in Ramoplanose

$i,i+1$ NOEs	Asn	Asn	HPG	Orn	Thr	HPG	HPG	Thr	Phe	Orn	HPG	Thr	HPG	Gly	Leu	Ala	CHP	(Asn2)
d_{NN}				–						–							–	–
$d_{\alpha N}$[a]	–	–	–		–	–	–	–	–	–	–	–	*	–	–	–		*
$d_{\text{side chain-N}}$	–	–	–	–	–		–	–		–	–	–	–	–		–	–	
$d_{\text{side chain-side chain}}$		–		–	–			–		–	–	–				–	–	

[a] Asterisks indicate that these $d^{\alpha}N$ connectivities were not observable due to saturation of the $C^{\alpha}H$ during the solvent suppression process.

Table V. Interresidue NOEs in Ramoplanose[a]

	1	2	3	4	5	6	7	8	9	10	11	12	13	14	15	16	17
1	O	X												X	X		
2	X	O	X											X			X
3		X	O	X			X						X				X
4			X	O	X							X	X				
5				X	O	X					X	X					
6					X	O	X				X	X					
			X			X	O	X		X	X						
8							X	O	X	X							
9								X	O	X							
10							X	X	X	O	X						
11					X	X	X			X	O	X					
12					X	X					X	O	X				
13			X	X								X	O	X			
14	X	X		X									X	O	X		
15	X													X	O	X	X
16															X	O	X
17		X	X												X	X	O

[a] X denotes that an NOE is observed between protons in the residues indicated on each axis.

(Table V). The off-diagonal elements indicate an antiparallel β-sheet structure for much of the antibiotic, while the intersection of diagonal and off-diagonal elements indicates turns in the vicinity of Thr8/Phe9 and Gly14/Ala15. The slow rate of exchange with solvent and low temperature coefficients of the amide protons of Thr5, HPG7, Orn10, Thr12, Gly14, and CHP17 are consistent with the hydrogen-bonding scheme present in this β-sheet (Figure 7).[34] Although the amide proton of β-OH(Asn2) showed similar characteristics, it was not initially obvious whether this was due to hydrogen bonding or poor solvent accessibility induced by the local fold of the peptide.

Distance geometry calculations were combined with restrained molecular dynamics to generate potential solution structures of ramoplanose according to the protocol detailed in the Experimental Section. Distance geometry calculations using DGEOM[22] did not converge when all NOE distance constraints were included, and the input structure included all carbon-bound protons. This was attributed to computational limitations. Reducing the set of distance constraints to those between amide NH, $C^{\alpha}H$, and $C^{\beta}H$ protons, and removing all protons except NH, $C^{\alpha}H$, and $C^{\beta}H$, made the problem more tractable, and a set of 20 structures were produced on which further calculations were performed. To check the quality of results generated by using this subset of constraints, the structure was divided into two overlapping sections (residues 4–14, and 12–6) and calculations using the complete set of NOE constraints for each section were performed. In both cases, calculations converged and the conformation of the overlapping residues was broadly comparable. Connected sections from these runs had a fold similar to that of structures generated from the limited constraint set, as judged by visual inspection and fit to NOE data, and it was concluded that the latter method of structure generation was acceptable in this case.

After restrained minimization in the AMBER force field, the quality of fit of the 20 structures to the NOE data was assessed. Those five structures which best satisfied the NOE data were subjected to restrained molecular dynamics according to the protocol described in the Experimental Section. In early runs, hydrogen-bonding constraints were not used in either distance geometry or dynamics calculations. The results of these runs were assessed in the light of the exchange rates and temperature coefficients of amide protons (Table II). These data were rationalized in terms of the hydrogen-bonding scheme proposed in Figure 7. The complete calculations were then repeated including

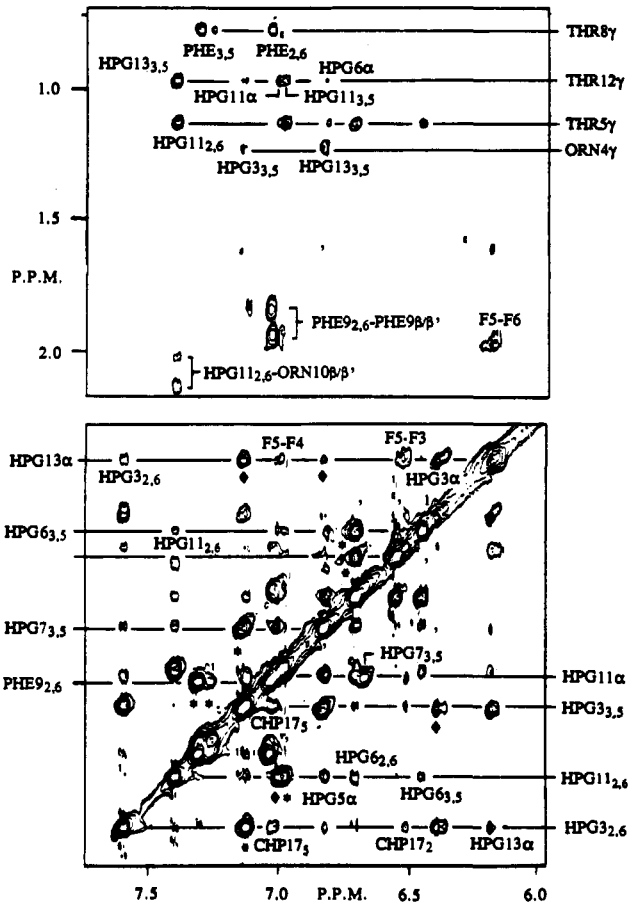

Figure 8. Two sections from a 500-MHz NOESY spectrum of ramoplanose in D_2O (mixing time 200 ms): (a) NOEs between aromatic and aliphatic side chains and (b) aromatic–aromatic side chain NOEs. Asterisk indicates a NOE to a ring proton within the same residue as the resonance labeled in the margin. A solid diamond indicates a NOE between ring protons of the residue labeled in the margin.

(34) (a) Kopple, K. D.; Ohnishi, M.; Go, N. *J. Am. Chem. Soc.* **1969**, *91*, 4264. (b) Ohnishi, M.; Urry, D. W. *Biochem. Biophys. Res. Commun.* **1969**, *36*, 194.

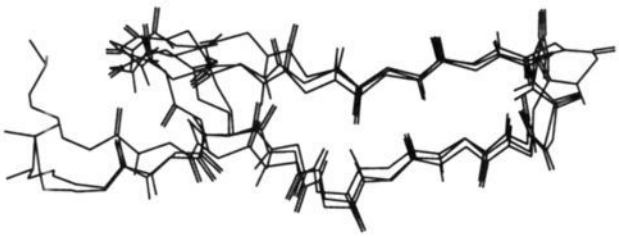

Figure 9. Superposition of backbone atoms of three out of five best calculated structures. Average RMSD between structures is 1.3 Å for backbone atoms. The largest pairwise RMSD for backbone atoms is 2.0 Å.

these seven hydrogen-bonding constraints (NH···O = 1.8–2.1 Å, N···O = 2.7–3.0 Å), and the quality of the structures produced was markedly improved, as judged by the fit to the NOE data. The origin of protection of β-OH(Asn2)NH was not evident from the initial calculations, and no hydrogen-bonding constraints were applied to this proton. The best refined structures showed excellent agreement with the NOE data, with no distance violation greater than 0.4 Å present in these structures. All peptide bonds were of trans conformation. The maximum RMSD between the backbone atoms of any two of the five structures was 2.0 Å. The average pairwise RMSD for backbone atoms was 1.3 Å, for side chain heavy atoms was 3.5 Å, and for all atoms was 3.2 Å. The average pairwise RMSD between all five structures and the set of averaged coordinates was 0.8 Å for backbone atoms. The backbone atoms of three of the five final structures are shown superimposed in Figure 9. Residues 5–12 form a standard section of antiparallel β-sheet containing a reverse β-turn between residues 7 and 10. The amide protons of Orn4 and Thr5 are both hydrogen-bonded to the carbonyl Gly14, with the former two residues forming a β-bulge.[35] Residues 14–17 also form a β-turn, in which CHP17 NH is protected from solvent exchange. There is a greater conformational variation in the turn regions, particularly at the C-terminal turn. The lactone linkage between β-OH(Asn2) and CHP17 adopts a cis conformation with the $CONH_2$ group of β-OH(Asn2) exo to the peptide macrocycle. Imposing hydrogen-bonding constraints in dynamics simulations as described above allowed the slow exchange behavior of β-OH(Asn2) amide to be rationalized, since a bifurcated hydrogen bond appears to be formed between the carbonyl of Leu15 and the NH protons of both β-OH(Asn2) and CHP17. The N-terminal fatty acid folds over the C-terminal β-turn to form a hydrophobic region with the side chains of Leu15 and Ala14.

Discussion

The primary structure determined for ramoplanose closely resembles that of ramoplanin A2[12-14] and to a lesser extent enduracidin.[36] Ramoplanin is isolated as a series of factors differing in the nature of the attached fatty acid (octadienoic, 7-methyloctadienoic, and 8-methylnonadienoic acid). However, in all cases the stereochemistry within the diene is cis–transoid–cis, differing from the cis–transoid–trans fatty acid found in the present study. The reported factors of ramoplanin contain only two mannose units, where ramoplanose contains an extra sugar attached to the 3-hydroxy group of MAN1. Such a variation in peripheral groups appears to be a common feature of peptide antibiotics.[3,4] These differences are, however, unlikely to affect significantly the solution conformation of the antibiotic.

The results described above clearly show that ramoplanose adopts a well-defined conformation in aqueous solution. The high quality (in terms of narrow line width and wide shift dispersion) of the NMR spectra obtained from aqueous solution is a strong indicator that the antibiotic adopts a stable, compact conformation in such an environment. In contrast to this, the poor quality of

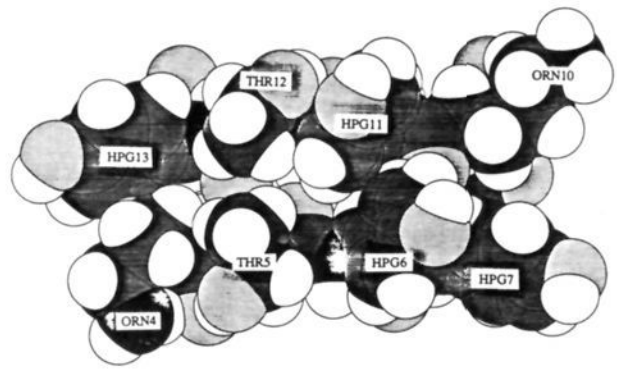

Figure 10. Residues 4–13 in the β-sheet showing side chain packing. Side chains of Thr8 and Phe9 are removed for clarity.

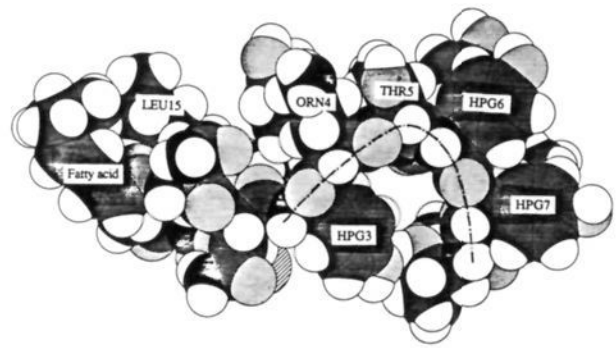

Figure 11. View of typical structure from the side showing the curvature of the sheet (broken line) and the cleft thus formed.

the spectra acquired in organic media (DMSO and DMSO/TFA mixtures) was rationalized in terms of solvent-induced aggregation or conformational hetereogeneity in the antibiotic.[12-14] Thus, it seems that the surrounding medium is important in stabilizing the conformation of the antibiotic. Furthermore, since the antibiotic acts against bacteria in an aqueous environment, we consider studies in aqueous solution to be of more relevance in drawing conclusions about the mode of action of the antibiotic. Further evidence of the stability of the solution conformation are the six amide protons that exchange slowly with the solvent. These resonances are present for 7–10 days after initial addition of D_2O at pH 4.0 and 300 K. Under similar conditions, amide protons in random coil structures typically have half-lives on the order of only minutes.[37] These data indicate that the antibiotic adopts a specific conformation in aqueous solution which is stabilized by intramolecular hydrogen bonds across the sheet. The bulky side chains may also serve to limit solvent access to these protons, retarding their exchange to an even greater extent.

We have noted that the presence of amino acids of D and L absolute stereochemistry makes the formation of helical structure unlikely. This mixing of stereochemistries may be used to prevent degradation by proteolytic enzymes. Attempts to cleave selectively peptide bonds with proteolytic enzymes to aid in the structure determination process were unsuccessful, presumably due to the D stereochemistry of certain residues (trypsin, α-chymotrypsin, and staphylococcus V8 protease digestions were attempted).

The stereochemistries of the amino acids in the β-sheet of ramoplanose also play a key role in determining the folded conformation of the antibiotic. Residues 10–15, forming one strand of the β-sheet, have alternating stereochemistry (D-L-D-L-Gly). Similarly, residues 5–7 alternate D-L-D in stereochemistry. Consequently, the side chains of residues 5–7, 10–12, and 13 are placed on the *same* side of the β-sheet (referred to as the "top" side, Figure 10). The β-bulge present at residue 4 also serves to position the side chain of Orn4 on this side of the sheet. The

(35) Richardson, J. S.; Getzoff, E. D.; Richardson, D. C. *Proc. Natl. Acad. Sci. U.S.A.* **1978**, *75*, 2574.

(36) (a) Hori, M.; Iwasaki, H.; Horii, S.; Yoshida, I.; Hongo, T. *Chem. Pharm. Bull.* **1973**, *21*, 1175. (b) Iwasaki, H.; Horii, S.; Asai, M.; Mizuno, K.; Ueyanagi, J.; Miyake, A. *Chem. Pharm. Bull.* **1973**, *21*, 1184.

(37) (a) Molday, R. S.; Englander, S. W.; Kallen, R. G. *Biochemistry* **1971**, *11*, 150. (b) Englander, D. B.; Calhoun, J. J.; Englander, S. W. *Anal. Biochem.* **1979**, *92*, 517.

sheer steric bulk of all these side chains on the top side of the molecule causes a pronounced bending of the sheet, the bottom face having a concave nature (see broken line in Figure 11). The aromatic ring of HPG3 partially fills the cleft thus formed.

The activity of ramoplanin against Gram-positive bacteria apparently involves inhibition of cell wall biosynthesis. The production of the cell wall precursor *N*-acetylglucosaminyl-*N*-acetylmuramyl-(pentapeptide)-pyrophosphate-undecaprenol from *N*-acetylmuramyl-(pentapeptide)-pyrophosphate-undecaprenol appears to be the site of inhibition (P. Reynolds, personal communication). In this respect, the cleft formed by the β-sheet in ramoplanose may be important for activity by binding to *N*-acetylmuramyl-(pentapeptide)-pyrophosphate-undecaprenol.

The formation of elements of regular secondary structure of high stability within ramoplanose is by no means the expected result for a peptide of this size. For example, studies on a fragment of atrial natriuretic factor (ANF7–23—containing 17 amino acids cyclized through a disulfide bond) have been reported recently.[38] In aqueous solution, fast amide proton exchange, lack of long-range NOEs, and $^3J_{\alpha NH}$ values indicative of conformational averaging all indicate an absence of well-defined secondary structure and allude to a random-coil-like condition of ANF7-23. Structure can be induced in ANF7-23 by the addition of SDS micelles,[39] but even in such an environment, the structure consists of a series of turns rather than continuous sections of regular secondary structure. Other cases where β-sheet formation has been proposed in small linear peptides may be a result of aggregation rather than the occurrence of real intramolecular secondary structure. In the absence of complete characterization of the sheet in terms of intramolecular cross-strand $d_{\alpha N}$, d_{NN}, and $d_{\alpha\alpha}$ NOEs, most other spectroscopic parameters (such as intense sequential $d_{\alpha N}$ NOEs, large $^3J_{NH\alpha}$ coupling constants, or β-strand-specific infrared or circular dichroism bands) could arise from intermolecular association rather than signifying well-folded monomeric units.[40]

The presence of 16 residues in the macrocycle places ramoplanose in a category different from smaller cyclic peptides such as gramicidin S. Gramicidin S does contain a section of antiparallel β-sheet,[41] but the range of accessible conformations is severely limited by the small ring size (10 residues) and by the presence of two proline residues that enforce turns at either end of the sheet.

Small sections of stable antiparallel β-sheet have been identified in synthetic peptides of single zinc finger (TFIIIA-type) domains,[42] and in a subfragment of bovine pancreatic trypsin inhibitor representing an independent folding domain.[43] Generally, these TFIIIA-type zinc finger peptides require divalent metal ions for folding,[44] and consist of 2–3 turns of helix packed against a section of antiparallel β-sheet. Similarly, the fragment from bovine pancreatic trypsin inhibitor contains an antiparallel β-sheet in intimate contact with a helical section (13 residues), the two being linked by a disulfide bridge. In both these examples, the β-sheet is not free standing, but is stabilized by a small hydrophobic core between sheet and helix. Presumably, the formation of this domain results in mutual stabilization of the helix and the sheet. In contrast, the β-sheet in ramoplanose exists freely in solution, without any requirement for packing against another element of secondary structure.

The β-sheet observed in ramoplanose, rigidly constrained by eight intramolecular backbone–backbone hydrogen bonds and protected from solvent by the packing of hydrophobic side chains, is apparently unique among small polypeptides. Formation of such a β-sheet is probably a consequence of two distinct factors. Firstly, the presence of a high proportion of residues branched at C^β (Thf, HPG) severely limits the accessible region of ϕ–ψ space.[45] Secondly, in forming the β-sheet, a large proportion of the hydrophobic regions of the Orn, Thr, and HPG side chains is removed from contact with solvent. The alteration of stereochemistries along the β-sheet backbone plays a crucial role in allowing this concentration of hydrophobic side chains, which presumably also protects the backbone–backbone hydrogen bonds from solvent. The hydrophilic termini of these residues ensure that the peptide remains soluble in an aqueous environment.

Acknowledgment. A Ramsay Memorial General British Fellowship is acknowledged by M.M.H., and R.J.M.S. thanks the SERC and Pfizer Ltd. for a CASE award. We thank Dr. Len Packman for carrying out the amino acid analyses, Dr. Mark Rance for providing the spectral simulation software (SPINNER), and Drs. Andrew Vinter, Mark Gardner, and Andrew Raine for helpful discussions. This work was carried out as part of the Cambridge Molecular Recognition Initiative.

(38) Fesik, S. W.; Holleman, W. H.; Perun, T. J. *Biochem. Biophys. Res. Commun.* **1985**, *131*, 517.
(39) Olejniczak, E. T.; Gampe, R. T.; Rockway, T. W.; Fesik, S. W. *Biochemistry* **1988**, *27*, 7124.
(40) For example, see: Muga, A.; Surewicz, W. K.; Wong, P. T. T.; Mantsch, H. H.; Singh, V. K.; Shinohara, T. *Biochemistry* **1990**, *29*, 2945.
(41) Stern, A.; Gibbons, W. C.; Craig, L. C. *Proc. Natl. Acad. Sci. U.S.A.* **1968**, *61*, 734.
(42) (a) Lee, M. S.; Gippert, G. P.; Soman, K. V.; Case, D. A.; Wright, P. E. *Science* **1989**, *245*, 635. (b) Pavletich, N. P.; Pabo, C. O. *Science* **1991**, *252*, 809.
(43) Oas, T. G.; Kim, P. S. *Nature* **1988**, *336*, 42.
(44) Lee, M. S.; Gottesfeld, J. M.; Wright, P. E. *FEBS Lett.* **1991**, *29*, 2925.
(45) Nemethy, G.; Leach, S. J.; Scheraga, H. A. *J. Phys. Chem.* **1966**, *70*, 998.